Inhibition of ATP-activated current by zinc in dorsal root ganglion neurones of bullfrog

Chaoying Li*, Robert W. Peoples and Forrest F. Weight

Laboratory of Molecular and Cellular Neurobiology, National Institute on Alcohol Abuse and Alcoholism, National Institutes of Health, Bethesda, MD 20892-8115, USA

1. The effect of Zn^{2+} on ATP-activated current was studied in bullfrog dorsal root ganglion (DRG) neurones using the whole-cell patch-clamp technique.

2. Zn^{2+} (2–800 μM) inhibited current activated by submaximal concentrations of ATP. The Zn^{2+} concentration that produced 50% inhibition (IC_{50}) of current activated by 2·5 μM ATP was 61 ± 9·8 μM. When ATP concentrations were adjusted to account for chelation of Zn^{2+}, the IC_{50} of Zn^{2+} was 86 ± 18 μM.

3. The inhibitory action of Zn^{2+} on ATP-gated channels did not appear to be due to a decrease in the concentration of one or more species of ATP.

4. Zn^{2+} inhibition of ATP-activated current was independent of membrane potential between −80 and +40 mV, and did not involve a shift in the reversal potential of the current.

5. Zn^{2+} (100 μM) shifted the ATP concentration–response curve to the right in a parallel manner, increasing the EC_{50} for ATP from 2·5 ± 0·5 μM to 5·5 ± 0·4 μM.

6. Zn^{2+} decreased the time constant of deactivation of ATP-gated ion channels without affecting the time constant of activation or desensitization.

7. Dithiothreitol (DTT) reversed Zn^{2+} inhibition of ATP-activated current.

8. 2-Methylthio ATP, α,β-methylene ATP and ADP activated current with EC_{50} values of 2·4 ± 0·3, 50·1 ± 5·8 and 303·1 ± 53·9 μM, respectively. Adenosine, AMP or β,γ-methylene ATP did not evoke detectable current.

9. Reactive Blue 2 and pyridoxal-phosphate-6-azophenyl-2′,4′-disulphonic acid inhibited ATP-activated current.

10. The results suggest that Zn^{2+} can inhibit P2X purinoceptor function by decreasing the affinity of the binding site for ATP. These observations provide the first evidence for this action of Zn^{2+} on a neurotransmitter-gated ion channel. Furthermore, the receptor–channel in these neurones appears to be a novel member of the P2X purinoceptor class.

The P2X purinoceptors are receptor–cation channels that are gated by extracellular ATP. Although the physiological role of these receptors has not been established, their potential importance is evidenced by their ability to mediate fast synaptic transmission and their widespread distribution in the nervous system. Activation of P2X purinoceptors elicits excitatory postsynaptic currents or excitatory postsynaptic potentials in the medial habenula of rat brain (Edwards, Gibb & Colquhoun, 1992) and in tissue cultures of autonomic ganglion neurones (Evans, Derkach & Surprenant, 1992; Silinsky, Gerzanich & Vanner, 1992) and myenteric ganglion neurones (Galligan & Bertrand, 1994), and elicits excitatory junction potentials in smooth muscle cells (Sneddon, Westfall & Fedan, 1982). In addition, P2X purinoceptor-mediated excitatory responses have been observed in many other types of peripheral neurones, including sensory (Krishtal, Marchenko & Pidoplichko, 1983; Bean, 1990; Bean, Williams & Ceelen, 1990; Li, Aguayo, Peoples & Weight, 1993*a*; Li, Peoples, Li & Weight, 1993*b*; Khakh, Humphrey & Surprenant, 1995; Robertson, Rae, Rowan & Kennedy, 1996), sympathetic (Cloues, Jones & Brown, 1993; Khakh *et al.* 1995) and parasympathetic neurones (Fieber & Adams, 1991), as well as in a number of central neurones (Ueno, Harata, Inoue &

* To whom correspondence should be addressed at the Laboratory of Molecular and Cellular Neurobiology, National Institute on Alcohol Abuse and Alcoholism, National Institutes of Health, 12501 Washington Avenue, Rockville, MD 20852, USA.

Akaike, 1992; Shen & North, 1993). Thus excitatory synaptic transmission mediated by these receptors may be widespread throughout the peripheral and central nervous systems.

Activation of P2X purinoceptors at negative membrane potentials induces an inward ion current, which shows inward rectification, non-selective cation permeability and a reversal potential close to 0 mV. Among various preparations, however, differences in the current–voltage relationships, agonist selectivity, desensitization (e.g. Khakh *et al.* 1995) and single-channel properties (Krishtal, Marchenko & Obukhov, 1988; Bean *et al.* 1990; Cloues, 1995; Wright & Li, 1995) of ATP-activated current have been observed, which are consistent with the existence of multiple subtypes of P2X purinoceptor–channels (Surprenant, Buell & North, 1995). Recent studies have also revealed that P2X purinoceptors in rat nodose ganglion neurones exhibit two different responses to physiological concentrations of Zn^{2+}: marked potentiation in the majority of neurones, but no effect in a subset of neurones (Li *et al.* 1993*b*; Li, Peoples & Weight, 1996). In contrast, we report in the present study that in dorsal root ganglion (DRG) neurones from the bullfrog, micromolar concentrations of Zn^{2+} inhibit P2X purinoceptor-mediated responses. This receptor–channel may thus represent a novel member of the P2X purinoceptor class. In addition, Zn^{2+} decreases the apparent affinity of ATP for the P2X receptor, and the effect of Zn^{2+} can be reversed by DTT, an agent that reduces sulfhydryl groups.

METHODS

Isolation of neurones

Freshly isolated neurones from bullfrog DRG were prepared as described previously (Li *et al.* 1993*a*). Briefly, adult male bullfrogs (*Rana catesbeiana*) were decapitated and both brain and spinal cord were destroyed by pithing. The care and use of animals in this study was approved by the Animal Care and Use Committee of the National Institute on Alcohol Abuse and Alcoholism (protocol no. LMCN-SP-01) in accordance with National Institutes of Health guidelines.

DRGs (usually 6) were rapidly isolated and transferred to a Petri dish containing Dulbecco's Modified Eagle's Medium (DMEM) (1·38 g DMEM and 0·2 g NaCl dissolved in 100 ml distilled water, pH 7·2, osmolality 260 mosmol kg^{-1}) and cut into small pieces. The DRG fragments were transferred to a flask containing 5 ml of DMEM in which trypsin III (0·55 mg ml^{-1}) and collagenase 1A (1·1 mg ml^{-1}) had been dissolved, and incubated at 35 °C for approximately 30 min in a shaking water bath. Trypsin digestion was stopped by the addition of soybean trypsin inhibitor I-S (1·8 mg ml^{-1}). Neurones were plated in 35 mm × 10 mm uncoated plastic Petri dishes and used for electrophysiological recording after at least 1 h, to allow for cell attachment. The neurones studied in this investigation were 30–55 μm in diameter.

Whole-cell patch-clamp recording

Neurones were observed under an inverted microscope (Diaphot, Nikon, Japan) using phase-contrast optics. Whole-cell patch-clamp recordings were carried out at room temperature using an EPC-7 (List Electronic) patch-clamp amplifier connected via a Labmaster TL-1 interface to a computer (Compaq 386/20e). Gigaohm seals were made using borosilicate glass microelectrodes (World Precision Instruments) with tip resistances of 2–4 MΩ. Data were filtered at 3 kHz, displayed on a digital oscilloscope (2090-IIIA, Nicolet Instrument Co., Madison, WI, USA) and recorded on a chart recorder (2400S, Gould Electronics). In experiments measuring onset, offset and desensitization rates (see below), data were filtered at 3 kHz, recorded on videotape using a VR-10B digital data recorder (Instrutech Corp., Great Neck, NY, USA) connected to a videocassette recorder (Sony SLV-440), and were later refiltered at 1 kHz and acquired at 2 kHz on a computer using pCLAMP software (Axon Instruments). Series resistance in all recordings was < 5 MΩ, and was compensated by 50–70%. Membrane potential was usually held at −60 mV, except where indicated.

Solutions and their application

The patch pipette (internal) solution contained (mM): 110 CsCl, 2 $MgCl_2$, 0·4 $CaCl_2$, 4·4 EGTA, 5 Hepes, 1·5 ATP; pH was buffered to 7·2 using CsOH and osmolality was adjusted to 240 mosmol kg^{-1} with sucrose when necessary. The free Ca^{2+} concentration in this solution was calculated to be 15 nM. The external solution contained (mM): 117 NaCl, 2 KCl, 2 $CaCl_2$, 2 $MgCl_2$, 5 Hepes, 10 D-glucose; pH was buffered to 7·2 using NaOH and osmolality was adjusted to 260 mosmol kg^{-1} with sucrose. Culture dishes containing neurones were continuously superfused at 1–2 ml min^{-1} with normal external solution. Drug solutions were prepared in extracellular medium. ATP, added as the Na^+ salt, was prepared daily. As extracellular pH can modulate the function of ATP-gated ion channels in the cells used in this study (Li, Peoples & Weight, 1997*a*), the pH of solutions was readjusted after addition of ATP or other drugs, as necessary.

Drug and agonist applications were performed using a modification of a superfusion system described previously by Johnson & Ascher (1987). We used a fourteen-barrelled array of perfusion pipettes composed of fused silica tubes, each with an internal diameter of ~200 μm. Drug solutions were delivered by gravity flow from independent reservoirs placed above the preparation, and solution changes were effected by shifting the pipette array horizontally using a micromanipulator (the 10–90% rise time of the junction potential at an open pipette tip was < 50 ms). Drug and agonist applications were spaced at least 2 min apart. Zn^{2+} or other agents were applied simultaneously with ATP, unless stated otherwise. Cells were constantly bathed in normal external solution flowing from one pipette barrel between agonist applications.

Rapid application of solutions

Measurement of rates of desensitization, onset and offset of ATP-activated current was performed using a system consisting of two 300 μm i.d. fused silica tubes set at ~30 deg angles to each other. Each of these exit tubes was connected to a manifold constructed from four barrels of 300 μm i.d. fused silica tubing glued together in a cylindrical pattern and inserted into a length (~5 mm) of Silicone rubber tubing (500 μm i.d.). Solution flowed continuously from one of the two exit tubes, and solutions were rapidly changed by closing and opening solenoid valves (The Lee Co., Westbrook, CT, USA) to switch the flow between the two exit tubes. Solenoid valves were controlled by computer using locally written software (VDriver; R. W. Peoples) to allow for rapid and precise opening and closing. This system allowed up to six treatment solutions to be applied (one of the four barrels in each manifold contained normal external solution). Using this system, the 10–90% rise time of the junction potential at an open pipette tip was ~2 ms.

Estimation of Zn^{2+} concentration

Concentration of free Zn^{2+} was estimated using the program Bound and Determined (Brooks & Storey, 1992), which compensates for variation in temperature, pH, and ionic strength. Values for Mn^{2+} were used as estimates of Zn^{2+} concentrations, since ATP has similar affinities for Mn^{2+} and Zn^{2+} (16 *vs.* 14 μM; Sillen & Martell, 1964), and the software does not directly calculate Zn^{2+} concentration. All concentrations of ATP and Zn^{2+} given are total concentrations unless stated otherwise.

Drugs and chemicals

All of the drugs, enzymes and chemicals used in these experiments were purchased from Sigma, except 2-methylthio ATP (2-MeSATP), α,β-methylene ATP (α,β-MeATP), β,γ-methylene ATP (β,γ-MeATP) and pyridoxal-phosphate-6-azophenyl-2′,4′-disulphonic acid (PPADS), which were purchased from Research Biochemicals International, and the salts, which were purchased from Mallinckrodt, Inc. (Paris, KY, USA).

Data analysis

Data were statistically compared using Student's t test or analysis of variance (ANOVA), as noted. Statistical analysis of concentration–response data was performed using the non-linear curve-fitting program ALLFIT (DeLean, Munson & Rodbard, 1978), which uses an ANOVA procedure. Values reported for concentrations yielding 50% inhibition (IC_{50}) or 50% of maximal effect (EC_{50}) and slope factor (n) are those obtained by fitting the data to the Hill equation:

$$Y = E_{max}/[1 + (IC_{50}/X)^n],$$

where X and Y are concentration and response, respectively, and E_{max} is the maximal response.

Current amplitudes reported are peak values, unless noted otherwise. Average values are expressed as means ± S.E.M., with n equal to the number of cells studied. The desensitization, activation and deactivation of current activated by ATP in the absence and presence of Zn^{2+} were fitted with a single-exponential function using the program NFIT (Island Products, Galveston, TX, USA).

RESULTS

Inhibition of ATP-activated current by Zn^{2+}

As illustrated in Fig. 1, inward current activated by extracellular ATP in bullfrog DRG neurones was inhibited by micromolar concentrations of Zn^{2+}. The amplitude of inward current activated by 2·5 μM ATP was markedly decreased in the presence of 50, 100 and 200 μM Zn^{2+} and completely recovered after Zn^{2+} washout (Fig. 1*A*). On average, 50, 100 and 200 μM Zn^{2+} decreased the amplitude of current activated by 2·5 μM ATP by 46 ± 4% ($n = 8$),

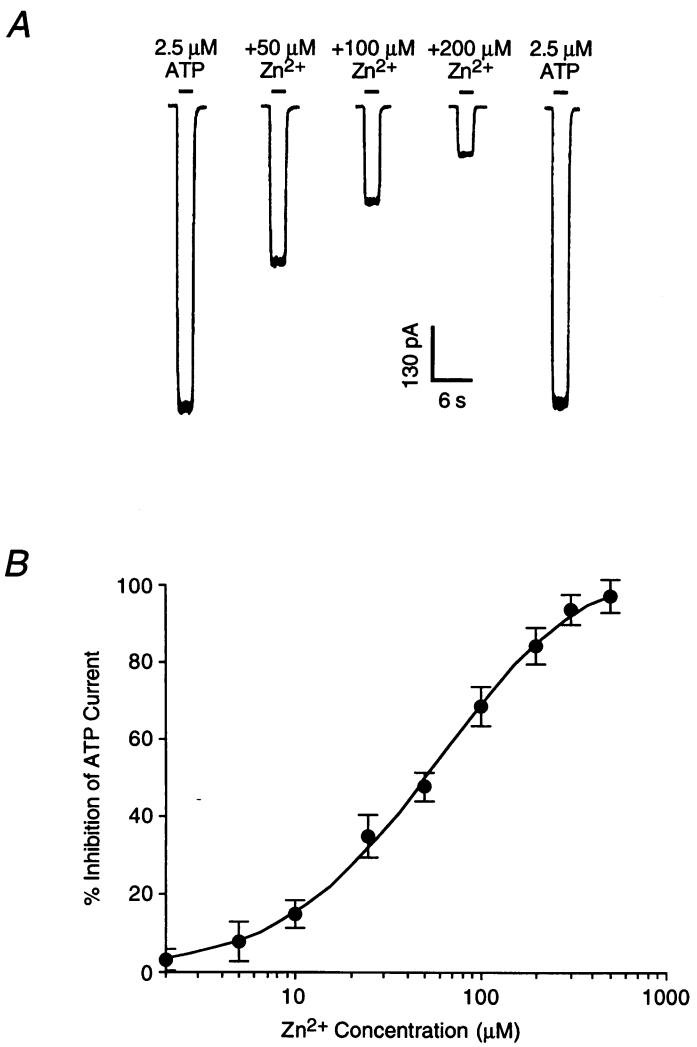

Figure 1. Inhibition of ATP-activated inward current by Zn^{2+}

A, records of current activated by 2·5 μM ATP in the presence of 50, 100 and 200 μM Zn^{2+}, respectively. Records are sequential current traces (from left to right) obtained from a single neurone. Bar above each record indicates time of agonist application in the absence or presence of different concentrations of Zn^{2+}, as labelled. *B*, average percentage inhibition of the amplitude of current activated by 2·5 μM ATP as a function of Zn^{2+} concentration. Each point is the average current from 5–11 cells. The curve shown is the best fit of the data to the equation described in Methods. Fitting the data to this equation yielded an IC_{50} of 61 ± 9·8 μM, a slope factor of 1 ± 0·2, and an E_{max} of 100 ± 8% of inhibition.

Table 1. Concentrations (μM) of major species of ATP in external solutions with different total concentrations of ATP and Zn^{2+}

Species	2·5 μM ATP	2·5 μM ATP + 200 μM Zn^{2+}	3·14 μM ATP + 200 μM Zn^{2+}
ATP (free)	0·09	0·072	0·09
NaATP	0·111	0·088	0·111
MgATP	1·252	0·996	1·251
MgHATP	0·003	0·002	0·003
CaATP	0·762	0·607	0·763
CaHATP	0·003	0·002	0·003
HATP	0·021	0·017	0·021
KATP	0·002	0·001	0·002
Mg_2ATP	0·07	0·056	0·07
Ca_2ATP	0·184	0·147	0·184
ZnHATP	—	$5·4 \times 10^{-4}$	$6·7 \times 10^{-4}$
ZnATP	—	0·51	0·64
ZnCl	—	22·716	22·701
Zn	—	176·774	176·658

Concentrations were determined using the program Bound and Determined, as described in the Methods. Species occurring at concentrations lower than 10^{-11} M are not shown.

68 ± 5% ($n = 11$) and 84 ± 6% ($n = 7$), respectively. Zn^{2+} inhibition of current activated by 2·5 μM ATP was observed in all neurones tested ($n = 108$), and exhibited a clear concentration dependence over the concentration range, 2–500 μM (Fig. 1*B*). The calculated Zn^{2+} concentration that produced 50% inhibition (IC_{50}) of current activated by 2·5 μM ATP was 61 ± 9·8 μM, the slope factor was 1 ± 0·2, and the maximal effect was 100 ± 8% inhibition. Over the concentration range of 2–800 μM, application of Zn^{2+} alone did not activate detectable current (data not shown).

Zn^{2+} inhibition and concentrations of various ATP species

As shown in Table 1, addition of 200 μM Zn^{2+} to the solution containing 2·5 μM ATP resulted in a decrease in the calculated concentrations of all species of ATP. This raised the possibility that the inhibitory effect of Zn^{2+} on ATP-activated current is due to a decrease in the concentration of one or more active forms of ATP, as has been proposed for Mg^{2+} inhibition of P2X purinoceptor function in PC12 cells (Choi & Kim, 1996). To test this possibility, we held constant the concentrations of all forms of ATP, except for ZnATP and ZnHATP, by increasing the total ATP concentration from 2·5 μM in the absence of Zn^{2+} to 3·14 μM in the presence of 200 μM Zn^{2+} (Table 1). Under these conditions, the current activated by 3·14 μM ATP in the presence of 200 μM Zn^{2+} was much smaller in amplitude than that activated by 2·5 μM ATP in the absence of Zn^{2+} (Student's *t* test, $P < 0·001$; $n = 5$; Fig. 2*A*).

Although 200 μM Zn^{2+} markedly inhibited ATP-activated current even when the ATP concentration was corrected for chelation of Zn^{2+}, the magnitude of the inhibition was less than that observed when the ATP concentration was not corrected (84 ± 6 *vs.* 66 ± 3·1% inhibition of current activated by 2·5 and 3·14 μM ATP, respectively). Based upon this observation, we determined the effect of chelation of Zn^{2+} by ATP on the Zn^{2+} concentration–response curve. Correction for the depletion of ATP due to chelation of Zn^{2+} yielded the Zn^{2+} concentration–response curve shown in Fig. 2*B* (continuous curve). All forms of ATP not bound to Zn^{2+} were held at 2·5 μM by increasing the ATP concentration as needed to correct for increases in Zn^{2+} concentration. At Zn^{2+} concentrations of 25 μM and below, depletion of ATP was negligible. The IC_{50} of Zn^{2+} for inhibition of ATP-activated current under these conditions was 86 ± 18 μM, the slope factor was 0·64 ± 0·15, and the maximal effect was 100% inhibition. The IC_{50}, slope and E_{max} values of this curve were not significantly different from those obtained when the ATP concentrations were not corrected to account for Zn^{2+} chelation (dashed curve; ANOVA, $P > 0·1$).

Voltage independence of Zn^{2+} inhibition of ATP-activated current

The voltage sensitivity of Zn^{2+} inhibition of ATP-activated current was examined by holding the membrane potential at a single voltage for > 1 min before activating current with ATP in the absence and presence of Zn^{2+}. As shown in Fig. 3*A*, current activated by 2·5 μM ATP in a typical neurone was smaller in amplitude at +40 mV than at −40 mV. The percentage inhibition of ATP-activated current in this cell by 100 μM Zn^{2+}, however, was similar at either membrane holding potential. On average, the percentage inhibition of ATP-activated current by 100 μM Zn^{2+} was

62 ± 5% at +40 mV and 67 ± 4% at −40 mV ($n = 5$). Figure 3*B* shows the current–voltage plot for 2·5 μM ATP-activated current in the absence and presence of 100 μM Zn^{2+} in the same neurone used to obtain the data shown in Fig. 3*A*. In this cell, Zn^{2+} produced a similar percentage reduction of amplitude of current activated by ATP at membrane voltages between +40 and −80 mV, and did not alter the reversal potential of ATP-activated current. In five out of five neurones tested, Zn^{2+} inhibited ATP-activated current in a voltage-independent manner (ANOVA, $P > 0{\cdot}25$), and did not significantly change the reversal potential of ATP-activated current (Student's t test, $P > 0{\cdot}25$).

Dependence of Zn^{2+} inhibition on ATP concentration

To examine whether the concentration of ATP affects Zn^{2+} inhibition, we performed the experiment shown in Fig. 4. The records in Fig. 4*A* show current activated by 1 μM ATP before, during and after application of 100 μM Zn^{2+} (upper series), and current activated by 10 μM ATP under the same conditions in the same cell (lower series). On average, 100 μM Zn^{2+} decreased the amplitude of the current activated by 1 and 10 μM ATP by 83 ± 5% ($n = 6$) and 23 ± 4% ($n = 5$), respectively. Figure 4*B* illustrates that Zn^{2+} shifted the ATP concentration–response curve to the right in a parallel manner. In the absence of Zn^{2+}, ATP had an EC_{50} of 2·5 ± 0·5 μM, a slope factor of 1·1 ± 0·2, and an E_{max} of 1. Zn^{2+} (100 μM), increased the EC_{50} of ATP to 5·5 ± 0·4 μM (ANOVA, $P < 0{\cdot}01$), but did not alter the slope factor (1·2 ± 0·13) or E_{max} (1·0 ± 0·03) of the curve ($P > 0{\cdot}5$). The preceding values were obtained when ATP concentrations were corrected to account for chelation of Zn^{2+} (continuous curve); the values obtained when ATP concentrations were uncorrected (dashed curve) did not differ significantly (EC_{50}, 6·3 ± 0·5; slope factor, 1·2 ± 0·1; E_{max}, 1 ± 0·03; ANOVA, $P > 0{\cdot}5$).

Effect of Zn^{2+} on receptor activation and deactivation

To examine further the mechanism of Zn^{2+} action on ATP-gated channels, we determined the activation and deactivation time constants for ATP-activated current in solutions with different Zn^{2+} concentrations. To allow accurate measurement of time constants within the limits of the fast perfusion system (time constant of 7 ± 1·2 ms for solution changes in patch-clamped cells; Fig. 5*A* inset), we used ATP concentrations of 2·5 μM or lower. To ensure that the measurement of the rates of activation and deactivation of the receptor by ATP was not influenced by the rates of

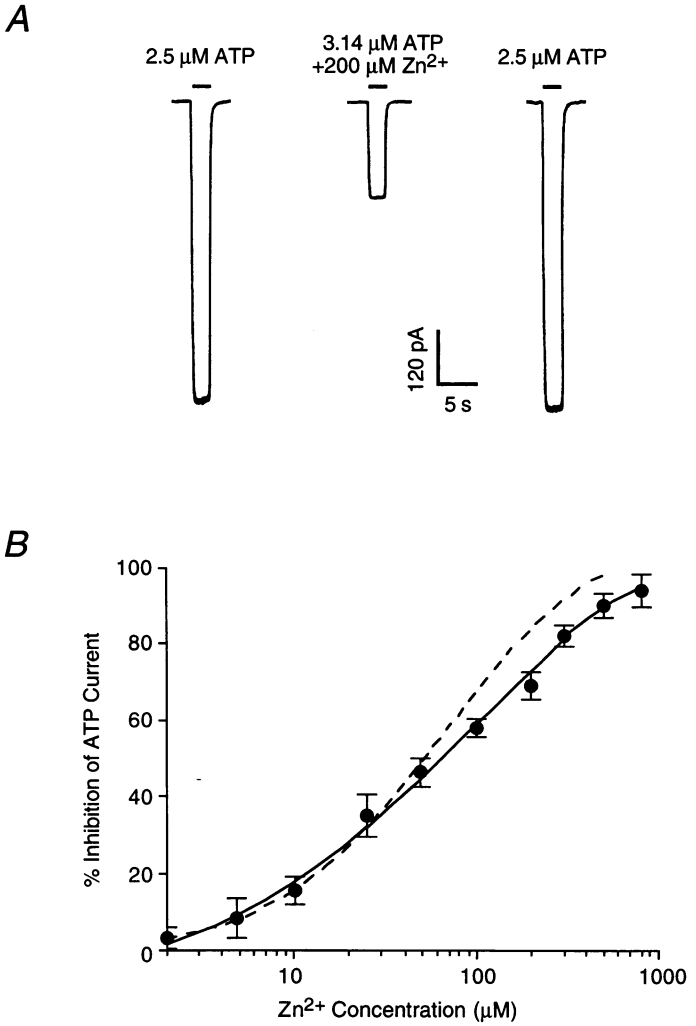

Figure 2. Effect of controlling concentrations of various forms of ATP on Zn^{2+} inhibition of ATP-activated current

A, currents activated by 2·5 μM ATP in normal external solution and by 3·14 μM ATP in the presence of 200 μM Zn^{2+} in a single neurone. Under these conditions, the calculated concentrations of all forms of ATP, except for ZnATP and ZnHATP, were held constant. Note that the current activated by 3·14 μM ATP in the presence of 200 μM Zn^{2+} was much smaller in amplitude than that activated by 2·5 μM ATP in normal external solution (240 ± 36 *vs.* 692 ± 23 pA, respectively; Student's t test, $P < 0{\cdot}001$; $n = 5$). *B*, average percentage inhibition of the amplitude of current activated by ATP as a function of Zn^{2+} concentration. For Zn^{2+} concentrations above 25 μM, the ATP concentration was adjusted to hold the concentration of ATP not bound to Zn^{2+} at 2·5 μM as follows: 50 μM Zn^{2+}, 2·66 μM ATP; 100 μM Zn^{2+}, 2·82 μM ATP; 200 μM Zn^{2+}, 3·14 μM ATP; 300 μM Zn^{2+}, 3·45 μM ATP; 500 μM Zn^{2+}, 4·1 μM ATP; 800 μM Zn^{2+}, 5·0 μM ATP. Amplitude of current activated by 2·5 μM ATP served as the control value for calculation of percentage inhibition. Each point is the average current from 4–7 cells. The continuous curve shown is the best fit of the data to the equation described in the Methods. Fitting the data to this equation yielded an IC_{50} of 86 ± 18 μM, a slope factor of 0·64 ± 0·15, and an E_{max} of 100 ± 17% of inhibition. The dashed curve was taken from Fig. 1*B* and is shown for comparison; the IC_{50}, slope, and E_{max} values of the two curves did not differ significantly (ANOVA, $P > 0{\cdot}1$).

onset and offset of Zn^{2+} action, we applied Zn^{2+} for 2 s before and after application of ATP. As shown in Fig. 5*A*, Zn^{2+} decreased the deactivation time constant (τ_{off}) of ATP-activated current from a control value of 180 ms in the absence of Zn^{2+} to 112 ms in the presence of 50 μM Zn^{2+}, and 100 μM Zn^{2+} produced a further decrease in τ_{off} to 35 ms. By contrast, Zn^{2+} did not appreciably change the activation time constant (τ_{on}). Activation time constants were highly dependent upon ATP concentration (ANOVA, $P < 0{\cdot}01$; $n = 6$), but were independent of Zn^{2+} concentration (ANOVA, $P > 0{\cdot}25$; $n = 6$; Fig. 5*B*). Deactivation time constants, however, were highly dependent upon Zn^{2+} concentration (ANOVA, $P < 0{\cdot}01$; $n = 6$), but were independent of ATP concentration (ANOVA, $P > 0{\cdot}25$; $n = 6$; Fig. 5*C*).

Effect of Zn^{2+} on receptor desensitization

To assess whether Zn^{2+} inhibits ATP-activated current by enhancement of receptor desensitization, we studied the desensitization of current activated by ATP in the absence and presence of 200 μM Zn^{2+}. As shown in Fig. 6*A*, the rate of decay of current activated by 20 μM ATP was decreased, rather than increased, by application of 200 μM Zn^{2+}. On average, the time constants of desensitization of current activated by 20 μM ATP were decreased significantly by 200 μM Zn^{2+} (Student's *t* test, $P < 0{\cdot}01$; $n = 5$), although the steady-state current amplitude was unaffected by Zn^{2+} (Student's *t* test, $P > 0{\cdot}1$; $n = 5$).

Zn^{2+} could decrease the decay rate of ATP-activated current by acting directly on the receptor–channel to decrease desensitization, or by decreasing the apparent concentration of ATP, indirectly resulting in a decrease in desensitization. To distinguish between these two possibilities, we examined the desensitization of current activated by a saturating concentration of ATP in the absence and the presence of 200 μM Zn^{2+}. Under these conditions, Zn^{2+} would not appreciably alter the apparent ATP concentration, and thus any change in the decay rate of the current should be attributable to a direct action of Zn^{2+} to decrease desensitization. From the traces shown in Fig. 6*B*, however, it can be seen that Zn^{2+} did not appreciably alter the desensitization rate or steady-state amplitude of the current activated by a saturating concentration (100 μM) of ATP in this neurone. On average, the time constant of desensitization and steady-state amplitude of current activated by 100 μM ATP were not significantly different in the absence and presence of 200 μM Zn^{2+} (Student's *t* test, $P > 0{\cdot}5$; $n = 5$).

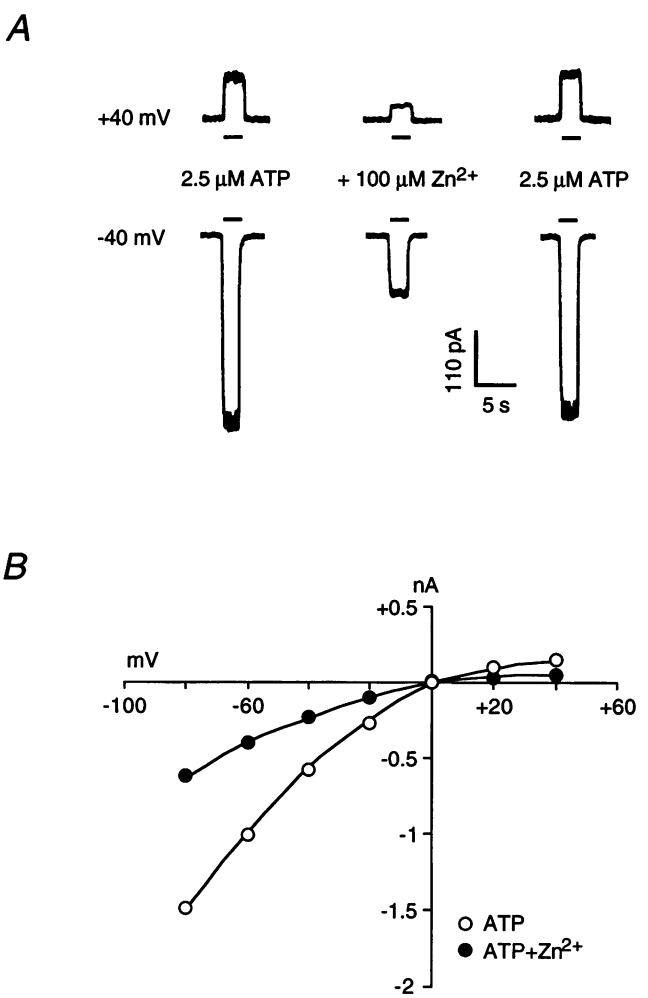

Figure 3. Effect of membrane potential on inhibition of ATP-activated current by Zn^{2+}

A, currents activated by 2·5 μM ATP before, during and after application of 100 μM Zn^{2+} in a single neurone voltage clamped at +40 mV (upper traces) and −40 mV (lower traces). Note that Zn^{2+} produced a similar percentage inhibition at both membrane potentials. *B*, current–voltage relationship (*I–V* plot) showing the amplitude of current activated by 2·5 μM ATP as a function of membrane potential, in the absence (○) and presence (●) of 100 μM Zn^{2+} in the same neurone from which data are shown in *A*. The reversal potential of current activated by 2·5 μM ATP was -1 ± 5 mV in the absence and 0 ± 7 mV in the presence of 100 μM Zn^{2+}; these values are not significantly different (Student's *t* test, $P > 0{\cdot}25$; $n = 5$). In addition, the percentage inhibition of ATP-activated current by Zn^{2+} was not significantly different at holding potentials from −80 to +40 mV (ANOVA, $P > 0{\cdot}25$; $n = 5$). In *A* and *B*, membrane potential was held at different levels for at least 1 min before evoking the current.

Effect of DTT on Zn^{2+} inhibition of ATP-activated current

The disulphide reducing reagent dithiothreitol (DTT) has been shown to affect the function of ligand-gated ion channels such as the *N*-methyl-D-aspartate (NMDA) receptor–ion channel complex. DTT potentiates NMDA-activated current (Aizenman, Lipton & Loring, 1989), and decreases the affinity of dynorphin for inhibition of NMDA receptors (Chen, Gu & Huang, 1995). Although ATP-activated current in the neurones used in this study was found to be insensitive to DTT treatment (Li *et al.* 1997*a*), we examined whether DTT could influence Zn^{2+} inhibition of this current. Figure 7 shows the effect of DTT treatment on Zn^{2+} inhibition of current activated by 2·5 and 100 μM ATP in an individual neurone. Zn^{2+} (200 μM) markedly inhibited current activated by 2·5 μM ATP in this neurone. Pretreatment of this cell for 2 min with 4 mM DTT, however, completely reversed Zn^{2+} inhibition of current activated by 2·5 μM ATP. Zn^{2+} (200 μM) had no effect on current activated by 100 μM ATP, as mentioned above, and DTT had no effect on current activated by 100 μM ATP in the presence of Zn^{2+}. In nine cells tested, DTT pretreatment decreased the percentage inhibition by 200 μM Zn^{2+} of current activated by 2·5 μM ATP from 81 ± 5% to 3·5 ± 2·1%.

Agonist and antagonist selectivity of ATP-gated receptor–ion channels

To characterize the pharmacological properties of ATP-gated receptor–ion channels in bullfrog DRG neurones, we examined the effects of several P2 purinoceptor agonists and antagonists. As shown in Fig. 8*A*, the P2 purinoceptor agonists 2-MeSATP, α,β-MeATP and ADP also evoked inward currents in these cells. Adenosine (10–800 μM; $n = 4$), AMP (10–800 μM; $n = 5$) and β,γ-MeATP (10–800 μM; $n = 4$) did not evoke detectable current (data not shown). The amplitude of inward current evoked by 2-MeSATP, α,β-MeATP and ADP was concentration dependent (Fig. 8*B*). Concentration–response analysis revealed that the maximal current evoked by 2-MeSATP did not differ significantly from that evoked by ATP (ANOVA, $P > 0{\cdot}1$), but the maximal current activated by α,β-MeATP was approximately 24% lower than that produced by ATP and 2-MeSATP (ANOVA, $P < 0{\cdot}005$). Maximal current activated by ADP was 2·7-fold lower than

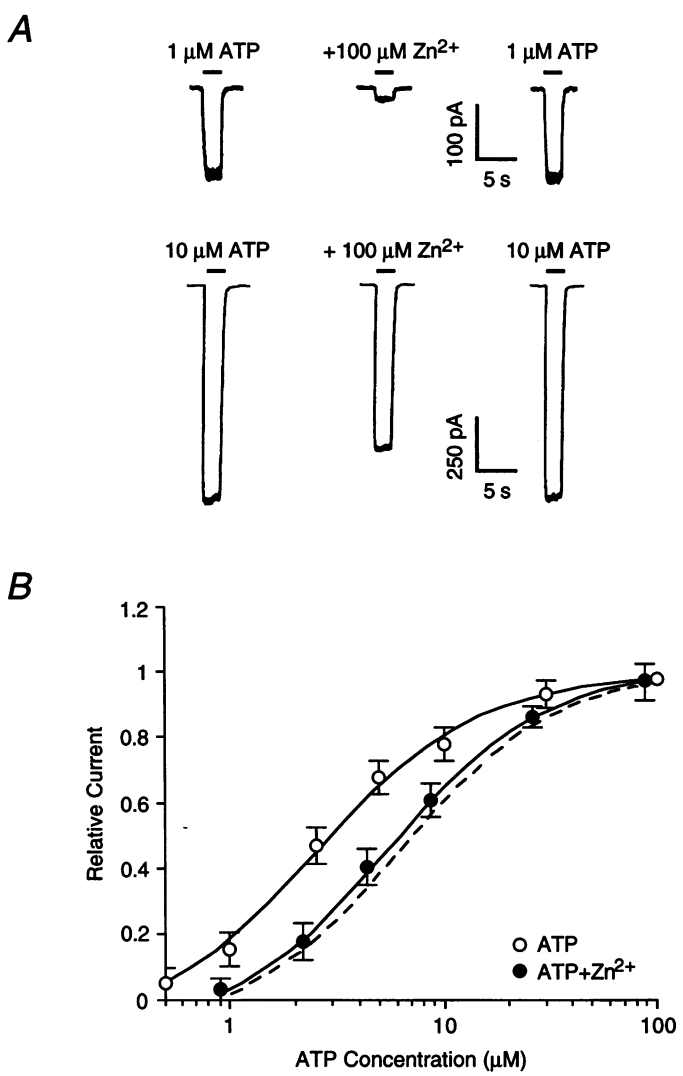

Figure 4. Effect of ATP concentration on Zn^{2+} inhibition of ATP-activated current

A, currents activated by 1 μM ATP (upper traces) and 10 μM ATP (lower traces) before, during and after application of 100 μM Zn^{2+} in a single neurone. *B*, relative amplitude of ATP-activated current in the absence (○) and presence (●) of 100 μM Zn^{2+} as a function of ATP concentration. Amplitude is normalized to the current activated by 100 μM ATP in the absence of Zn^{2+}. Each data point is the average current from 5–8 cells. The continuous curves shown are the best fits of the data to the equation described in the Methods. Zn^{2+} significantly increased the EC_{50} for ATP from 2·5 ± 0·5 μM in the absence of Zn^{2+} to 5·5 ± 0·4 μM in the presence of 100 μM Zn^{2+} (ANOVA, $P < 0{\cdot}01$). ATP concentrations in the presence of Zn^{2+} were corrected to account for chelation by Zn^{2+}. The dashed curve shown is the fit of the uncorrected data to the equation given in the Methods.

that of ATP. Values of EC_{50} and slope factor obtained from concentration–response analysis were 2·4 ± 0·3 μM and 1·1 ± 0·1 for 2-MeSATP, 50·1 ± 5·8 μM and 1·8 ± 0·5 for α,β-MeATP, and 303·1 ± 53·9 μM and 1·5 ± 0·2 for ADP, respectively. The slope factor values of ATP, 2-MeSATP, α,β-MeATP and ADP did not differ significantly from one another (ANOVA, $P > 0·5$). In contrast, there were clear differences in potency among the various agonists tested. Although the EC_{50} value for 2-MeSATP did not differ significantly from that of ATP (ANOVA, $P > 0·5$), α,β-MeATP was less potent than ATP (ANOVA, $P > 0·001$), and ADP was less potent than α,β-MeATP (ANOVA, $P > 0·001$). Thus, the order of agonist potency in these cells was 2-MeSATP = ATP > α,β-MeATP > ADP.

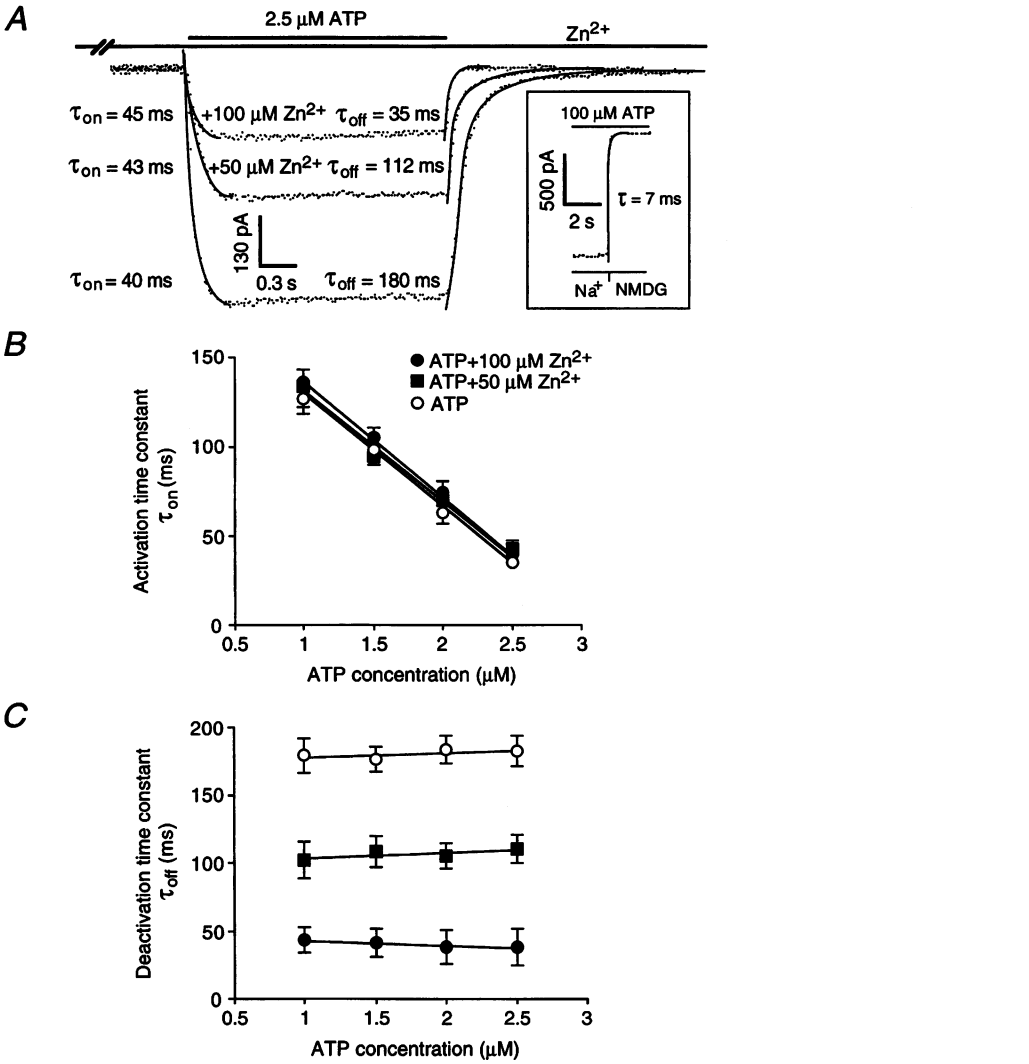

Figure 5. Effect of Zn^{2+} on activation and deactivation time constants of ATP-activated current
A, records of currents activated by 2·5 μM ATP in the absence and presence of 50 and 100 μM Zn^{2+}. Both activation and deactivation of the current were well fitted using single-exponential equations (continuous curves). To ensure that the measurement of the rates of activation and deactivation of the receptor by ATP was not influenced by the rates of onset and offset of Zn^{2+} action, we applied Zn^{2+} for 2 s before and after application of ATP. The activation time constant (τ_{on}) and deactivation time constant (τ_{off}) values in *A* are those obtained for the records shown. Note that both 50 and 100 μM Zn^{2+} had relatively little effect on τ_{on}, but greatly decreased τ_{off}. The inset shows the time constant for solution change in a patch-clamped cell. The solution bathing the cell was abruptly changed from normal external solution containing 100 μM ATP to the same solution with Na^+ replaced by an equimolar concentration of *N*-methyl-D-glucamine (NMDG). *B*, graph plotting average τ_{on} values as a function of ATP concentration in the absence (○), and presence of 50 (■) and 100 μM (●) Zn^{2+}. The average τ_{on} of ATP-activated current was highly dependent upon ATP concentration (ANOVA, $P < 0·01$; $n = 6$), but was independent of Zn^{2+} (ANOVA, $P > 0·25$; $n = 6$). *C*, graph plotting average τ_{off} values as a function of ATP concentration in the absence (○), and presence of 50 (■) and 100 μM (●) Zn^{2+}. The average τ_{off} of ATP-activated current was highly dependent upon Zn^{2+} (ANOVA, $P < 0·01$; $n = 6$), but was independent of ATP concentration (ANOVA, $P > 0·25$; $n = 6$).

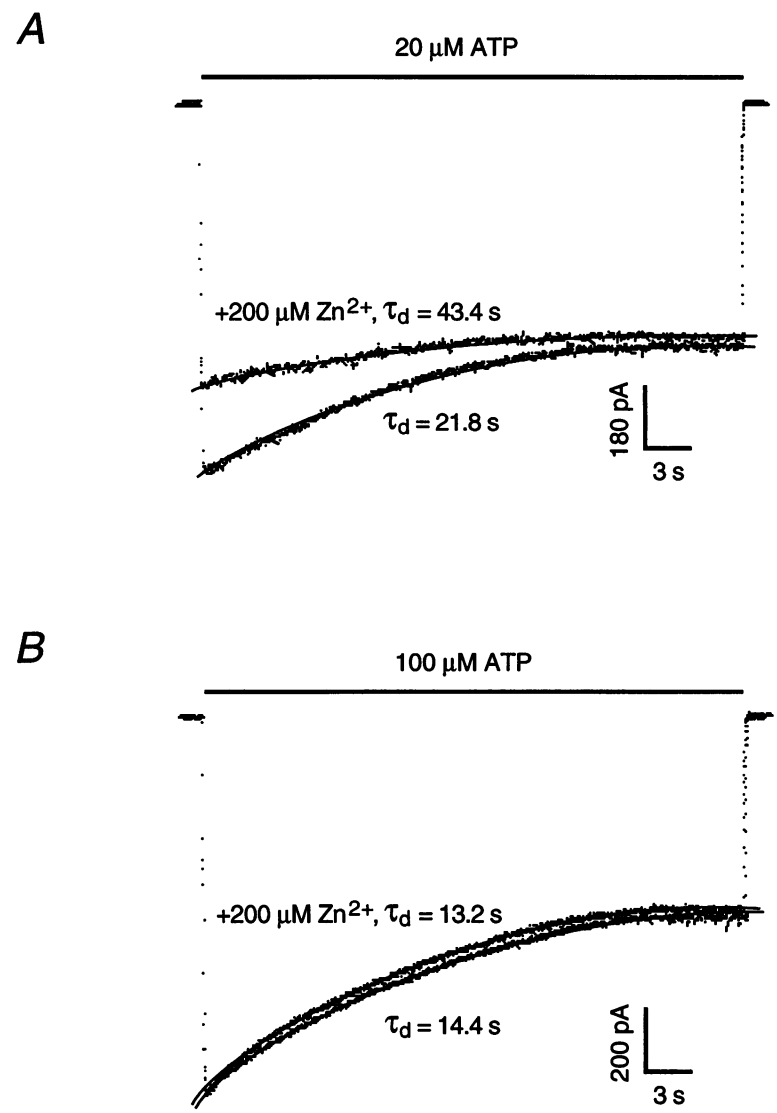

Figure 6. Effect of Zn^{2+} on desensitization of ATP-activated current

A, current traces illustrating the time constants of desensitization (τ_d) of current activated by 20 μM ATP in the absence and presence of 200 μM Zn^{2+}. The τ_d values in *A* are those obtained for the records shown. The average values of τ_d of current activated by 20 μM ATP were 22·4 ± 2·6 s and 44·2 ± 2·7 s in the absence and presence of 200 μM Zn^{2+}, respectively; these values are significantly different (Student's *t* test, $P < 0{\cdot}01$; $n = 5$). *B*, current traces illustrating the τ_d of currents activated by 100 μM ATP, a saturating concentration, in the absence and presence of 200 μM Zn^{2+} in the same cell from which data are shown in *A*. The τ_d values in *B* are those obtained for the records shown. The average values of τ_d of current activated by 100 μM ATP in the absence and presence of 200 μM Zn^{2+} were not significantly different (14·2 ± 2 s *vs.* 13·4 ± 3 s, respectively; Student's *t* test, $P > 0{\cdot}5$; $n = 5$). Desensitization of the ATP-activated currents in *A* and *B* was well fitted using a single-exponential equation (continuous curves).

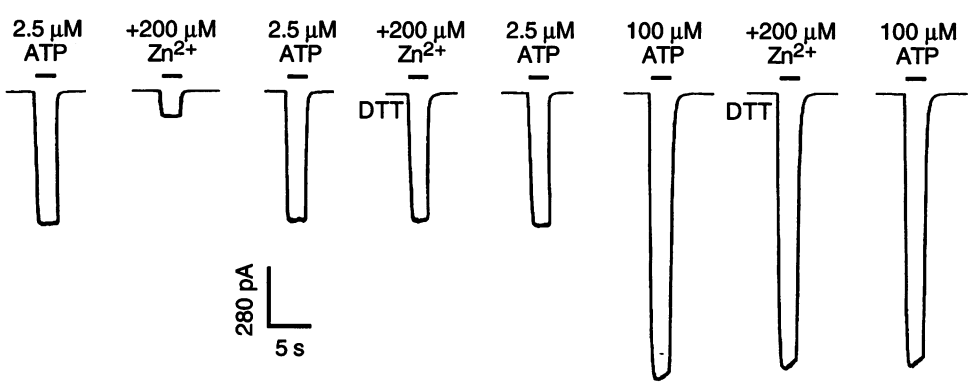

Figure 7. Effect of DTT on Zn^{2+} inhibition of ATP-activated current

Records of current activated by 2·5 and 100 μM ATP in the absence and the presence of 200 μM Zn^{2+} and their modulation by DTT. DTT (4 mM) was applied for 2 min prior to application of ATP and Zn^{2+}. Traces are sequential (from left to right) responses in a single neurone. Note that DTT reversed Zn^{2+} inhibition of current activated by 2·5 μM ATP.

We have previously reported that the P2 purinoceptor antagonist suramin effectively blocked ATP-activated current in bullfrog DRG neurones (Li *et al.* 1993*a*, 1997*a*). Figure 8*C* illustrates that the P2 purinoceptor antagonists Reactive Blue 2 and PPADS (Abbracchio & Burnstock, 1994) also markedly reduced the amplitude of ATP-activated current. Similar results were observed in five of five neurones tested (data not shown).

DISCUSSION

Previous studies have shown that Zn^{2+}, at micromolar concentrations, potentiates the function of P2X purinoceptors in various types of neurones (Cloues *et al.* 1993; Li *et al.* 1993*b*). In the present study, we found that the inward current activated by ATP in bullfrog DRG neurones was inhibited by Zn^{2+}. The effect of Zn^{2+} was concentration dependent, with a 50% inhibitory concentration (IC_{50}) of 61 μM for current activated by 2·5 μM ATP. When the chelation of Zn^{2+} by ATP was taken into account, the IC_{50} of Zn^{2+} was 86 μM.

Evidence for a direct interaction of Zn^{2+} with ATP-gated ion channels

Divalent cations, such as Mg^{2+}, have been proposed to inhibit the function of P2X purinoceptors by decreasing the putative active form of ATP, ATP^{4-} (Choi & Kim, 1996). In the present study, however, three lines of evidence support a direct interaction of Zn^{2+} with a site on ATP-gated ion channels rather than with the ATP molecule. First, holding the concentrations of the various forms of ATP (with the exception of ZnATP and ZnHATP) constant, by increasing the ATP concentration from 2·5 to 3·14 μM as the Zn^{2+} concentration was increased from 0 to 200 μM did not prevent Zn^{2+} inhibition of ATP-activated current. Thus, because a change in concentration of one or more forms of ATP does not appear to account for the effect of Zn^{2+}, the

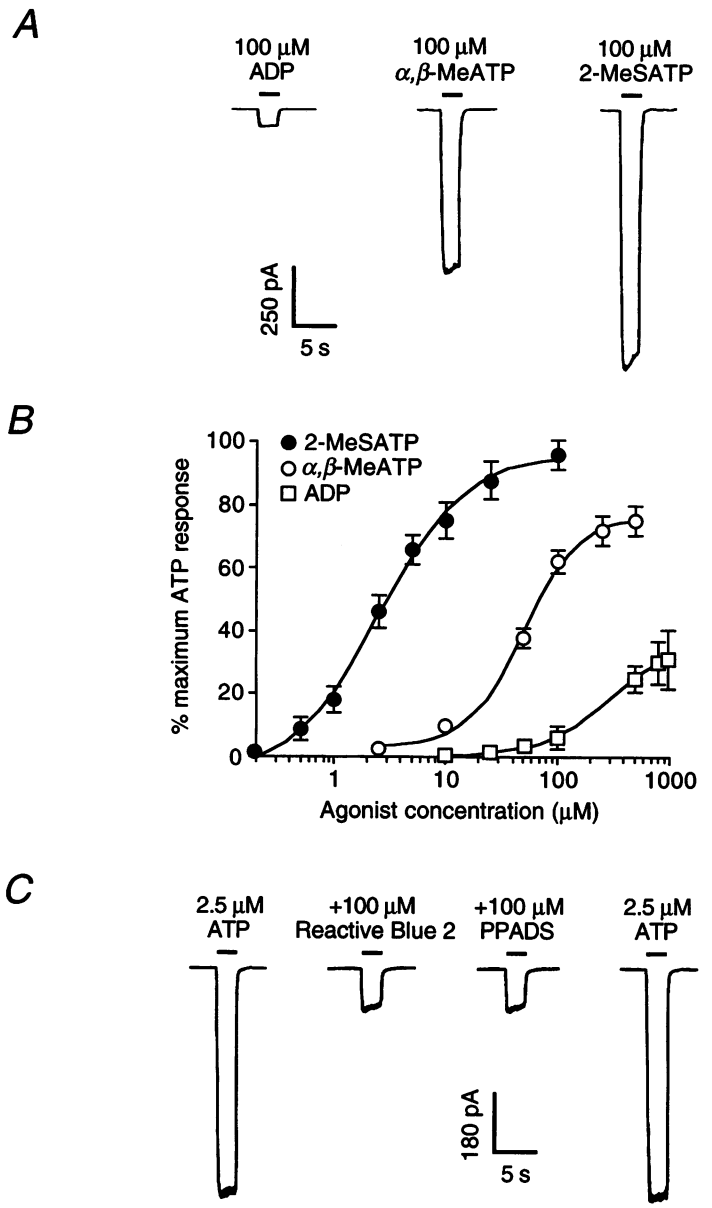

Figure 8. Effect of P2 agonists and antagonists on ATP-gated receptor–ion channels

A, sequential current responses (from left to right) to application of 100 μM ADP, α,β-MeATP and 2-MeSATP in a single neurone. *B*, relative amplitude of current activated by ADP (□), α,β-MeATP (○) and 2-MeSATP (●) as a function of agonist concentration. Amplitude is normalized to the current activated by 100 μM ATP. Each data point is the average current from 5–7 cells; error bars not visible are smaller than the size of the symbols. The curves shown are the best fits of the data to the equation described in the Methods. Fitting the data to this equation yielded the following values for ADP, α,β-MeATP and 2-MeSATP, respectively: EC_{50} values of 303·1 ± 53·9 μM, 50·1 ± 5·8 μM and 2·4 ± 0·3 μM; slope factor values of 1·5 ± 0·2, 1·8 ± 0·5 and 1·1 ± 0·1; and E_{max} values of 36·9 ± 3·2%, 76·5 ± 3·5% and 96·2 ± 2·9% of current activated by 100 μM ATP. *C*, current activated by 2·5 μM ATP in the presence of 100 μM Reactive Blue 2 or PPADS. Records are sequential current traces (from left to right) obtained from a single neurone.

primary effect of Zn^{2+} is attributable to a direct interaction with the receptor–channel. Secondly, Zn^{2+} did not change the apparent activation rate of ATP-gated channels. As a decrease in the agonist concentration will decrease the activation rate of the receptor–ion channel (Bean, 1990; Khakh *et al.* 1995; Li *et al.* 1997*a*), this observation is not consistent with a decrease in one or more active forms of ATP. Finally, the observation that the disulphide reducing agent DTT, which does not change the response to ATP (Li *et al.* 1997*a*), was able to reverse the effect of Zn^{2+} is not compatible with an action of Zn^{2+} mediated by a change in the concentration of one or more ATP species. Thus these observations are best explained by a direct interaction of Zn^{2+} with the ATP-gated receptor–channel.

Modulation of Zn^{2+} action by DTT

The reducing reagent DTT has been reported to modulate the function of neurotransmitter-gated ion channels, such as NMDA receptor–channels (Sullivan, Traynelis, Chen, Escobar, Heinemann & Lipton, 1994), by breaking disulphide bonds formed by cysteine residues. We have previously shown that DTT has no effect on the amplitude of ATP-activated current in the neurones used in this study (Li *et al.* 1997*a*). Despite the lack of effect of DTT on ATP-activated current in the absence of Zn^{2+}, Zn^{2+} inhibition of ATP-activated current in the present study could be completely reversed by treatment of the cells with DTT. This finding suggests that Zn^{2+} acts at a site on the ATP receptor–channel distinct from the agonist binding site. This observation might also appear to indicate that the site of action of Zn^{2+} contains one or more disulphide bonds between pairs of cysteine residues, and that these bonds are required for Zn^{2+} inhibition. The site of Zn^{2+} action could well contain one or more cysteine residues, as Zn^{2+} binding sites on proteins are composed of cysteine and histidine residues (Christianson, 1991). Because Zn^{2+} binds to the sulfhydryl groups of cysteine residues (Christianson, 1991), however, DTT would be predicted to enhance the effect of Zn^{2+}. Thus, it appears more probable that one or more disulphide bonds between cysteine residues outside of the Zn^{2+} binding site modulate its function by an allosteric action. As the amino acid sequence of the ATP-gated channel in the neurones used in the present study has not been determined, the identity of the cysteine residue or residues responsible for modulation of Zn^{2+} inhibition of ATP-gated receptors remains to be elucidated.

Mechanism of Zn^{2+} inhibition of ATP-gated channels

Mechanisms of receptor inhibition may be broadly classified as competitive, in which the antagonist and the agonist cannot be simultaneously bound to the receptor, and non-competitive, in which the antagonist and the agonist may simultaneously act on the receptor. Non-competitive inhibition encompasses a range of mechanisms, including open-channel block and enhancement of desensitization. Since Zn^{2+} is a cation, open-channel block would be a possible mechanism of inhibition of ATP-gated channels. Open-channel block by cationic molecules is usually voltage-dependent (Hille, 1992), but Zn^{2+} inhibition of ATP-activated current in the present study was independent of membrane voltage. This would not rule out the possibility of an open-channel block mechanism, however, as Zn^{2+} could bind to a site within the ion channel but beyond the influence of the membrane electrical field (Hille, 1992). This is unlikely, however, as Zn^{2+} inhibition can be overcome by increasing the concentration of ATP. Zn^{2+} might also alter the ion permeance ratio of ATP-gated channels, but because Zn^{2+} did not alter the reversal potential of current activated by ATP, this mechanism does not appear to account for the Zn^{2+} inhibition observed in the present study. Another possible mechanism for Zn^{2+} inhibition is enhancement of receptor desensitization. However, the observation that Zn^{2+} decreased, rather than increased, the rate of desensitization of current activated by a sub-maximal concentration of ATP, and did not alter the desensitization rate of current activated by a maximal concentration (100 μM) of ATP, makes this mechanism appear unlikely. Finally, concentration–response analysis revealed that Zn^{2+} did not alter the maximal response to ATP, which is consistent with either competitive inhibition or allosteric modulation affecting agonist binding.

Zn^{2+} shifted the ATP concentration–response curve to the right in a parallel manner, increasing the EC_{50} for ATP. A similar rightward shift of the agonist concentration–response curve by Zn^{2+} has been observed for 5-hydroxytryptamine 3 (5-HT_3; Lovinger, 1991) and γ-aminobutyric acid A ($GABA_A$; Yakushiji, Tokutomi, Akaike & Carpenter, 1987) neurotransmitter-gated ion channels. However, Zn^{2+} could produce such an effect by at least two different mechanisms: by competitive inhibition or by interaction with an allosteric site on the receptor–channel that results in a decrease in the affinity of the receptor for ATP. The latter mechanism has been reported for $GABA_A$ receptor inhibition by inverse agonists at the benzodiazepine site (Kemp, Marshall, Wong & Woodruff, 1987), and for inhibition of P2X purinoceptors by Mg^{2+} (Li, Peoples & Weight, 1997*b*). To distinguish between these possible mechanisms, we investigated the effect of Zn^{2+} on the activation and deactivation rates of ATP-gated channels. A competitive antagonist will decrease the activation rate of the receptor–ion channel without changing its deactivation rate (Clements & Westbrook, 1994), whereas an antagonist that decreases the affinity of the receptor for agonist will increase the deactivation rate without changing its activation rate (Li *et al.* 1997*b*). In the present study, we found that Zn^{2+} did not affect the activation rate of ATP-gated channels, but increased the deactivation rate. This observation is thus not consistent with competitive antagonism, but can be explained by a decrease in the affinity of the receptor for agonist via an action at an allosteric site. In addition, the observation that DTT, which does not alter the effect of ATP (Li *et al.* 1997*a*), reverses Zn^{2+} inhibition is difficult to reconcile with a competitive mechanism of inhibition, but is consistent with an allosteric action of Zn^{2+}.

Agonist and antagonist actions on P2X purinoceptors

The P2 purinoceptors have been classified into several subtypes based on the potency of agonists. Originally, the rank order of agonist potency for P2X purinoceptors was reported to be α,β-MeATP $\gg$ 2-MeSATP $\geqslant$ ATP (Kennedy & Leff, 1995). This classification was based largely on studies with a range of agonists performed in intact, multicellular organs. It was subsequently found that in many tissues ATP and 2-MeSATP, but not α,β-MeATP, are rapidly broken down by ectonucleotidases, and that when this enzymatic degradation is prevented, then 2-MeSATP and ATP are more potent than α,β-MeATP at P2X purinoceptors (Kennedy & Leff, 1995). Thus the corrected rank order of agonist potency for P2X purinoceptors is: 2-MeSATP $\geqslant$ ATP > α,β-MeATP. In the present study, we obtained an order of agonist potency for P2X purinoceptors of 2-MeSATP = ATP > α,β-MeATP > ADP. Thus, the agonist responses of the ATP-gated receptor–channels present on the neurones used in this study are typical of P2X purinoceptors. In addition, we obtained this order of potency in the absence of ectonucleotidase inhibitors, which suggests that minimal enzymatic degradation occurs under the conditions used in these experiments.

The inward current activated by ATP on the neurones used in this study has been reported to be inhibited by the non-specific purinoceptor antagonist suramin (Li *et al.* 1993*a*, 1997*a*). In the present study, we found that the P2 purinoceptor antagonists Reactive Blue 2 and PPADS also inhibited ATP-activated current. The inhibition of ATP-activated current by PPADS in the present study is in agreement with the classification of PPADS as a P2X purinoceptor antagonist (Abbracchio & Burnstock, 1994). PPADS does not appear to be selective for P2X receptors, however, as it has also recently been reported to inhibit endothelial P2Y purinoceptors (Brown, Tanna & Boarder, 1995). Similarly, Reactive Blue 2 has been classified as a putative P2Y purinoceptor antagonist (Abbracchio & Burnstock, 1994), but the present study and recent studies in neurones from rat nodose, rat superior cervical and guinea-pig coeliac ganglia (Khakh *et al.* 1995) show that it is also an effective antagonist for P2X purinoceptors. Thus, although the ATP-gated receptor–channels present on the neurones used in this study are inhibited by P2 purinoceptor antagonists, these antagonists are not selective for P2X purinoceptors. At present, classification of P2 purinoceptors therefore depends primarily on determination of order of agonist potency.

Despite similarities in order of agonist potency (Khakh *et al.* 1995; Robertson *et al.* 1996), the various P2X purinoceptors that have been identified in neurones differ in their desensitization kinetics, current–voltage relationships (e.g. Khakh *et al.* 1995), and single-channel properties (Krishtal *et al.* 1988; Bean *et al.* 1990; Cloues, 1995; Wright & Li, 1995). In addition, previous studies have indicated that P2X purinoceptors differ in their sensitivity to the agonist α,β-MeATP. In some cell types, such as rat nodose ganglion neurones, α,β-MeATP is as efficacious as ATP, but is less potent (Khakh *et al.* 1995), whereas in other cell types, such as rat superior cervical ganglion (SCG) neurones, α,β-MeATP has no agonist activity (Khakh *et al.* 1995). Based upon our previous observations and the observations in the present study, P2X purinoceptors also appear to be heterogeneous with respect to modulation by Zn^{2+}. In rat nodose ganglion neurones, P2X purinoceptors exhibit two different responses to physiological concentrations of Zn^{2+}: marked potentiation in the majority of neurones, but no effect in a subset of neurones (Li *et al.* 1993*b*, 1996). We now report that physiological concentrations of Zn^{2+} inhibit P2X purinoceptors in bullfrog DRG neurones. This receptor thus represents a novel member of the P2X purinoceptor class. Interestingly, Zn^{2+} modulation and α,β-MeATP sensitivity are, at least in part, independent of each other. For example, Zn^{2+} can potentiate ATP-activated current in rat nodose ganglion neurones (Li *et al.* 1993*b*) and rat SCG neurones (Cloues *et al.* 1993; Li *et al.* 1993*b*), but these cell types differ in their sensitivity to α,β-MeATP. Furthermore, in α,β-MeATP-sensitive neurones, Zn^{2+} can potentiate, inhibit, or have no effect on ATP-activated current. Whether Zn^{2+} can have multiple effects on α,β-MeATP-insensitive P2X purinoceptors is not known at present. As specific agonists and antagonists for the various P2X receptors have not been identified, modulation by Zn^{2+} should provide an additional criterion for their classification.

Abbracchio, M. P. & Burnstock, G. (1994). Purinoceptors: are there families of P2X and P2Y purinoceptors? *Pharmacology and Therapeutics* **64**, 445–475.

Aizenman, E., Lipton, S. A. & Loring, R. H. (1989). Selective modulation of NMDA responses by reduction and oxidation. *Neuron* **2**, 1257–1263.

Bean, B. P. (1990). ATP-activated channels in rat and bullfrog sensory neurons: concentration dependence and kinetics. *Journal of Neuroscience* **10**, 1–10.

Bean, B. P., Williams, C. A. & Ceelen, P. W. (1990). ATP-activated channels in rat and bullfrog sensory neurons: current-voltage relation and single-channel behavior. *Journal of Neuroscience* **10**, 11–19.

Brooks, S. P. J. & Storey, K. B. (1992). Bound and determined: a computer program for making buffers of defined ion concentrations. *Analytical Biochemistry* **201**, 119–126.

Brown, C., Tanna, B. & Boarder, M. R. (1995). PPADS: an antagonist at endothelial P_{2Y}-purinoceptors but not P_{2U}-purinoceptors. *British Journal of Pharmacology* **116**, 2413–2416.

Chen, L., Gu, Y. & Huang, L.-Y. M. (1995). The mechanism of action for the block of NMDA receptor channels by the opioid peptide dynorphin. *Journal of Neuroscience* **15**, 4602–4611.

Choi, S.-Y. & Kim, K.-T. (1996). Characterization of Na^+ influx mediated by ATP^{4-}-activated P_2 purinoceptors in PC12 cells. *British Journal of Pharmacology* **118**, 935–940.

Christianson, D. W. (1991). Structural biology of zinc. *Advances in Protein Chemistry* **42**, 281–355.

CLEMENTS, J. D. & WESTBROOK, G. L. (1994). Kinetics of AP5 dissociation from NMDA receptors: evidence for two identical cooperative binding sites. *Journal of Neurophysiology* **71**, 2566–2569.

CLOUES, R. (1995). Properties of ATP-gated channels recorded from rat sympathetic neurons: voltage dependence and regulation by Zn^{2+} ions. *Journal of Neurophysiology* **73**, 312–319.

CLOUES, R., JONES, S. & BROWN, D. A. (1993). Zn^{2+} potentiates ATP-activated currents in rat sympathetic neurons. *Pflügers Archiv* **424**, 152–158.

DELEAN, A., MUNSON, P. J. & RODBARD, D. (1978). Simultaneous analysis of families of sigmoidal curves: application to bioassay, radioligand assay, and physiological dose-response curves. *American Journal of Physiology* **235**, E97–102.

EDWARDS, F. A., GIBB, A. J. & COLQUHOUN, D. (1992). ATP receptor-mediated synaptic currents in the central nervous system. *Nature* **395**, 144–147.

EVANS, R., DERKACH, V. & SURPRENANT, A. (1992). ATP mediates fast synaptic transmission in mammalian neurons. *Nature* **357**, 503–505.

FIEBER, L. A. & ADAMS, D. J. (1991). Adenosine triphosphate-evoked currents in cultured neurones dissociated from rat parasympathetic cardiac ganglia. *Journal of Physiology* **434**, 239–256.

GALLIGAN, J. J. & BERTRAND, P. P. (1994). ATP mediates fast synaptic potentials in enteric neurons. *Journal of Neuroscience* **14**, 7563–7571.

HILLE, B. (1992). *Ionic Channels of Excitable Membranes.* Sinauer Associates, Sunderland, MA, USA.

JOHNSON, J. W. & ASCHER, P. (1987). Glycine potentiates the NMDA response in cultured mouse brain neurons. *Nature* **325**, 529–531.

KEMP, J. A., MARSHALL, G. R., WONG, E. H. F. & WOODRUFF, G. N. (1987). The affinities, potencies and efficacies of some benzodiazepine-receptor agonists, antagonists and inverse-agonists at rat hippocampal $GABA_A$-receptors. *British Journal of Pharmacology* **91**, 601–608.

KENNEDY, C. & LEFF, P. (1995). How should P2X purinoceptors be classified pharmacologically? *Trends in Pharmacological Sciences* **16**, 168–174.

KHAKH, B. S., HUMPHREY, P. P. A. & SURPRENANT, A. (1995). Electrophysiological properties of P_{2X}-purinoceptors in rat superior cervical, nodose and guinea-pig coeliac neurones. *Journal of Physiology* **484**, 385–395.

KRISHTAL, O. A., MARCHENKO, S. M. & OBUKHOV, A. G. (1988). Cationic channels activated by extracellular ATP in rat sensory neurons. *Neuroscience* **27**, 995–1000.

KRISHTAL, O. A., MARCHENKO, S. M. & PIDOPLICHKO, V. I. (1983). Receptor for ATP in the membrane of mammalian sensory neurons. *Neuroscience Letters* **35**, 41–45.

LI, C., AGUAYO, L., PEOPLES, R. W. & WEIGHT, F. F. (1993*a*). Ethanol inhibits a neuronal ATP-gated ion channel. *Molecular Pharmacology* **44**, 871–875.

LI, C., PEOPLES, R. W., LI, Z. & WEIGHT, F. F. (1993*b*). Zn^{2+} potentiates excitatory action of ATP on mammalian neurons. *Proceedings of the National Academy of Sciences of the USA* **90**, 8264–8267.

LI, C., PEOPLES, R. W. & WEIGHT, F. F. (1996). Cu^{2+} potently enhances ATP-activated current in rat nodose ganglion neurons. *Neuroscience Letters* **219**, 45–48.

LI, C., PEOPLES, R. W. & WEIGHT, F. F. (1997*a*). Enhancement of ATP-activated current by protons in dorsal root ganglion neurons. *Pflügers Archiv* **433**, 446–454.

LI, C., PEOPLES, R. W. & WEIGHT, F. F. (1997*b*). Mg^{2+} inhibition of ATP-activated current in rat nodose ganglion neurons: evidence that Mg^{2+} decreases the agonist affinity of the receptor. *Journal of Neurophysiology* **77**, 3391–3395.

LOVINGER, D. M. (1991). Inhibition of 5-HT_3 receptor-mediated ion current by divalent metal cations in NCB-20 neuroblastoma cells. *Journal of Neurophysiology* **66**, 1329–1337.

ROBERTSON, S. J., RAE, M. G., ROWAN, E. G. & KENNEDY, C. (1996). Characterization of a P_{2X}-purinoceptor in cultured neurones of the rat dorsal root ganglia. *British Journal of Pharmacology* **118**, 951–956.

SHEN, K.-Z. & NORTH, R. A. (1993). Excitation of rat locus coeruleus neurons by adenosine 5′-triphosphate: ionic mechanism and receptor characterization. *Journal of Neuroscience* **13**, 894–899.

SILINSKY, E. M., GERZANICH, V. & VANNER, S. M. (1992). ATP mediates excitatory synaptic transmission in mammalian neurones. *British Journal of Pharmacology* **106**, 762–763.

SILLEN, L. G. & MARTELL, A. E. (1964). *Stability Constants.* Chemical Society, London.

SNEDDON, P., WESTFALL, D. P. & FEDAN, J. S. (1982). Cotransmitters in the motor nerves of the guinea pig vas deferens: electrophysiological evidence. *Science* **218**, 693–695.

SULLIVAN, J. M., TRAYNELIS, S. F., CHEN, H.-S. V., ESCOBAR, W., HEINEMANN, S. F. & LIPTON, S. A. (1994). Identification of two cysteine residues that are required for redox modulation of the NMDA subtype of glutamate receptor. *Neuron* **13**, 929–936.

SURPRENANT, A., BUELL, G. & NORTH, R. A. (1995). P_{2X} receptors bring new structure to ligand-gated ion channels. *Trends in Neurosciences* **18**, 224–229.

UENO, S., HARATA, N., INOUE, K. & AKAIKE, N. (1992). ATP-gated current in dissociated rat nucleus solitarii neurons. *Journal of Neurophysiology* **68**, 778–785.

WRIGHT, J. M. & LI, C. (1995). Zn^{2+} potentiates steady-state ATP activated currents in rat nodose ganglion neurons by increasing the burst duration of a 35 pS channel. *Neuroscience Letters* **193**, 177–180.

YAKUSHIJI, T., TOKUTOMI, N., AKAIKE, N. & CARPENTER, D. O. (1987). Antagonists of GABA responses, studied using internally perfused frog dorsal root ganglion neurons. *Neuroscience* **22**, 1123–1133.

Author's email address

C. Li: cli@niaaa.nih.gov

Received 21 April 1997; accepted 8 August 1997.